FLOW AND HEAT TRANSFER OVER A STRETCHING SURFACE WITH VARIABLE THICKNESS IN A MAXWELL FLUID AND POROUS MEDIUM WITH RADIATION

by

Elsayed M. A. ELBASHBESHY [a], ***Hamada G. ASKER*** [b*], ***and Khaled M. ABDELGABER*** [b]

[a] Mathematics Department, Faculty of Science, Ain Shams University, Abbassia, Cairo, Egypt
[b] Department of Physics and Engineering Mathematics,
Faculty of Engineering - Mataria, Helwan University, Cairo, Egypt

Original scientific paper
https://doi.org/10.2298/TSCI170228146E

The effect of thermal radiation on flow and heat transfer of Maxwell fluid over a stretching surface with variable thickness embedded in a porous medium is considered. The governing non-linear PDE are transformed into a non-linear ODE by using a similarity transformation. These equations were solved numerically with fourth/fifth-order Runge-Kutta method. A comparison of obtained numerical results is made with the previously results in some special cases and excellent agreement is noted. The effects of elasticity, radiation parameter, porosity parameter, wall thickness parameter, and thermal conductivity parameter on the velocity and temperature profiles are presented. Moreover, the skin-friction and Nusselt number are presented.

Key words: *Maxwell fluid, variable thickness, stretching surface, thermal radiation, porous medium*

Introduction

Stretching surface in a stationary cooling fluid is the main stage in a lot of manufacturing processes such as plastic sheets, glass manufacturing, *etc.* At low enough values for the velocity ratio, Sakiadis [1] studied the Blasius flow showing that an increase in viscous dissipation enhances greatly the local heat transfer leading to temperature overshoots adjacent to the wall. Crane [2] extended the Sakiadis' work [1] considering the main velocity of outer flow is proportional to the distance from the stagnation point. The study presented rules approximating the temperature and the skin friction as a function of Prandtl number. Elbashbeshy and Bazid [3] showed that the dimensionless heat transfer coefficient decreases with increasing the velocity and decreasing the heat flux. Hossain *et al.* [4] investigated the effect of the thermal radiation on free convection flow of fluid with variable viscosity from a porous vertical plate showing that the local Nusselt number increases with increasing the local suction parameter. Cortell [5] claimed that the skin-friction parameter is independent of both Prandtl number and source/sink parameter while the permeability parameter increases the skin-friction and decreases the velocity. Also, the suction increases the velocity in contrary to the blowing effect. Yusof *et al.* [6] concluded that the heat transfer rate increases with unsteadiness parameter and Prandtl number and decreases with the radiation parameter and magnetic parameter. Elbashbeshy *et al.* [7] claimed

* Corresponding author, e-mail: asker_hamada@yahoo.com

that the skin-friction and Nusselt number increase with the dimensionless co-ordinates, thermal radiation, and heat generation/absorption parameter while they decrease with the Prandtl number and magnetic field. Mandal and Swati [8] repeated the work of Elbashbeshy *et al.* [7] in a porous medium where the shear stress surface increases with the permeability parameter.

Elbashbeshy *et al.* [9] studied the unsteady flow of Maxwell fluid showing that the modified skin friction increases with the elasticity parameter, magnetic field, and material parameter. Hsiao [10] used the improved parameters control method to investigate the effects of the electrical MHD ohmic dissipation forced and free convection on the Maxwell fluid with a stagnation point. The study created an applicable model in manufacturing processes. Furthermore, Hsiao [11] extended the previous study for a viscoelastic non-Newtonian Carreau-nanofluid on a stagnation point. Shehzad *et al.* [12] included the effect of the thermal radiation on the steady flow of Maxwell fluid over a flat surface in a porous medium then Waheed [13] repeated the work of Shehzad *et al.* [12] for an unsteady flow. Their studies showed that the temperature decreases with Prandtl number and increases with the elasticity parameter, while Noor *et al.* [14] presented a good approach to the effect of the internal heat sink on the heat transfer process. Hsiao [15] showed that increasing the magnetic parameter causes a decrease in the velocity, Nusselt number, in contrary to the material parameter. Also, increasing Prandtl number increases the temperature. Furthermore, Hsiao [16, 17] showed that increasing the free convection parameter decreases the temperature due to increasing the thermal boundary thickness.

Fang *et al.* [18] presented the non-flatness effect on the boundary-layer development along the stretching surface. Khader and Megahed [19], Khader *et al.* [20], and Eid and Khader [21] repeated the previous study including the thermal radiation, viscous dissipation, and MHD effects. Elbashbeshy *et al.* [22] studied the flow and heat transfer over a moving surface with variable thickness in a nanofluid in the presence of thermal radiation. The study showed that increasing the power index decreases the velocity in the boundary-layer near the surface, then returns to increasing it. Abdel-Wahed *et al.* [23] extended the previous work to present the effect of the non-flatness on the mechanical properties of the stretching surface such that the increasing of shape parameter produces a negative effect on the surface mechanical properties. Sulochana and Sandeep [24] studied the forced convection flow of a nanofluid showing that the thermal boundary-layer thickness becomes high in the presence of velocity slip. Also, the skin friction and the Nusselt number become small by increasing the magnetic field parameter. The flow of Maxwell fluid over a stretching surface with variable thickness is also considered by Hayat *et al.* [25].

The most previous studies discussed the boundary-layer flow over a flat surface, the others studied the effect of variable thickness (non-flatness) for the Newtonian fluids [18], for nanofluid [23], and for Maxwell fluid [25]. The aim of the present work is to discuss the characteristics of the fluid-flow and heat transfer of a Maxwell fluid over a steady moving surface with a variable thickness on the mechanical properties of the surface in the presence of porous media and thermal radiation during the heat treatment process.

Mathematical formulation

Consider a steady, laminar, and 2-D boundary-layer flow of Maxwell fluid over a stretching surface embedded in a porous medium. The surface profile is described with $y = a(x + b)^{(1-n)/2}$ and the stretching velocity is $U_w = a(x + b)^n$ as mentioned in [13, 26] where a and b are constants used to define the wall thickness at the slit ($x = 0$), the coefficient a is assumed to be very small so that the surface is sufficiently thin [23], and n – the velocity power index. The surface is assumed to be impermeable.

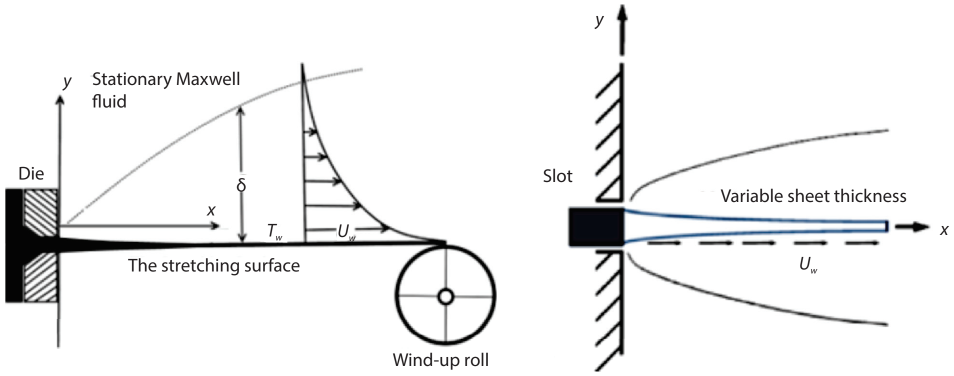

Figure 1. Schematic for flow above stretching surface

The schematic of the process is shown in fig. 1. The axis is chosen along the stretching surface in the direction of the motion and y-axis is taken normal to it. The thermal radiation is included in the energy equation. As mentioned in [13, 26], the equations governing the flow:

$$\frac{\partial u}{\partial x}+\frac{\partial \upsilon}{\partial y}=0 \tag{1}$$

$$u\frac{\partial u}{\partial x}+\upsilon\frac{\partial u}{\partial y}+\lambda_1\left[u^2\left(\frac{\partial^2 u}{\partial x^2}\right)+\upsilon^2\left(\frac{\partial^2 u}{\partial y^2}\right)+2u\upsilon\left(\frac{\partial^2 u}{\partial x\partial y}\right)\right]=\nu\frac{\partial^2 u}{\partial y^2}-\frac{\nu}{K}u \tag{2}$$

$$\rho C_p\left(u\frac{\partial T}{\partial x}+\upsilon\frac{\partial T}{\partial y}\right)=\frac{\partial}{\partial y}\left(k\frac{\partial T}{\partial y}\right)-\frac{\partial q_r}{\partial y} \tag{3}$$

subject to the boundary conditions:

$$\begin{gathered}u=U_w=a\left(x+b\right)^n,\ \upsilon=0,\ T=T_w\quad \text{at}\quad y=a\left(x+b\right)^{(1-n)/2}\\ u\to 0,\ T\to T_\infty\quad \text{as}\quad y\to\infty\end{gathered} \tag{4}$$

where $K = K_0(x + b)^{1-n}$ is the permeability of the porous medium. The fluid is considered to be gray absorbing-emitting radiation, but in a non-scattering medium, as mentioned in [3, 13, 27]. The Rosseland approximation simplifies the radiative heat flux q_r in the energy, eq. (3):

$$q_r=-\frac{4\sigma^*}{3k^*}\frac{\partial T^4}{\partial y} \tag{5}$$

where σ^* is the Stefan-Boltzmann constant and k^* – the mean absorption coefficient [13, 28]. Such as Rapits [28], considering that the temperature differences within the flow is sufficiently small such that T^4 may be expressed as a linear function of the temperature. Expanding T^4 by Taylor expansion about T_∞ and neglecting higher-order terms:

$$T^4=4T_\infty^3T-3T_\infty^4 \tag{6}$$

substituting eqs. (5) and (6) in the energy eq. (3):

$$\rho C_p\left(u\frac{\partial T}{\partial x}+\upsilon\frac{\partial T}{\partial y}\right)=\frac{\partial}{\partial y}\left(K_{eff}\frac{\partial T}{\partial y}\right) \tag{7}$$

where $K_{eff} = k + 16\sigma^*T_\infty^3/3k^*$ is the effective thermal conductivity.

The mathematical analysis of the problem is simplified by introducing the following dimensionless variables [23, 25, 26]:

$$\xi = y\sqrt{\left(\frac{n+1}{2}\right)\frac{a\left(x+b\right)^{n-1}}{\nu}},\ \psi = \sqrt{\frac{2}{n+1}\nu a\left(x+b\right)^{n+1}}F\left(\xi\right),\ \theta\left(\xi\right) = \frac{T-T_\infty}{T_w-T_\infty} \tag{8}$$

where $F(\xi)$ and $\theta(\xi)$ are dimensionless functions. Equations (2) and (7) are transformed into ODE using the similarity transformation technique. The equation of continuity:

$$u = \frac{\partial\psi}{\partial y},\quad \upsilon = \frac{\partial\psi}{\partial x} \tag{9}$$

The thermal conductivity is generalized [12, 20, 29]:

$$k = k_\infty\left(1+\varepsilon\theta\right) \tag{10}$$

where ε is the thermal conductivity parameter and k_∞ – the ambient thermal conductivity. Substituting eqs. (8)-(10) into eqs. (2) and (7) obtains the following ODE:

$$F''' + FF'' - \frac{2n}{n+1}F'^2 + \beta\left[\left(3n-1\right)FF'F'' - \frac{2n\left(n-1\right)}{n+1}F'^3 + \frac{n-1}{2}\eta F'^2F'' - \frac{n+1}{2}F^2F'''\right] - \lambda F' = 0 \tag{11}$$

$$\frac{1+R}{\mathrm{Pr}}\left[\left(1+\varepsilon\theta\right)\theta'' + \varepsilon\theta'^2\right] + F\theta' - \frac{2n}{n+1}F'\theta = 0 \tag{12}$$

with boundary conditions:

$$f\left(\alpha\right) = \alpha\left(\frac{1-n}{1+n}\right),\ f'(\alpha) = 1,\ \theta(\alpha) = 1,\ f''(\infty)\to 0,\ \theta(\infty)\to 0 \tag{13}$$

where $\beta = \lambda_1(x + b)^{n-1}$ is the elasticity number, $\lambda = 2\nu/ak_0(n + 1)$ – the porous parameter, $R = 16\sigma^*T_\infty^3/(3k^*k_\infty)$ – the radiation parameter, $\mathrm{Pr} = \mu C_p/k_\infty$ – the Prandtl number, $\alpha = a[a(n + 1)/2\nu]^{1/2}$ – the wall thickness parameter which describes the wall profile of the stretched surface, and $\xi = \alpha$ describes the surface profile. Let $F(\xi) = f(\xi - \alpha) = f(\eta)$ and $\theta(\xi) = \theta(\xi - \alpha) = \theta(\eta)$. Therefore, the similarity eqs. (11) and (12) in combined with the boundary conditions (13):

$$f''' + ff'' - \frac{2n}{n+1}f'^2 + \beta\left[\left(3n-1\right)ff'f'' - \frac{2n\left(n-1\right)}{n+1}f'^3 + \frac{n-1}{2}\eta f'^2f'' - \frac{n+1}{2}f^2f'''\right] - \lambda f' = 0 \tag{14}$$

$$\frac{1+R}{\mathrm{Pr}}\left[\left(1+\varepsilon\theta\right)\theta'' + \varepsilon\theta'^2\right] + f\theta' - \frac{2n}{n+1}f'\theta = 0 \tag{15}$$

with boundary conditions:

$$f\left(0\right) = \alpha\left(\frac{1-n}{1+n}\right),\ f'(0) = 1,\ \theta(0) = 1,\ \ f'(\infty)\to 0,\ \theta(\infty)\to 0 \tag{16}$$

The local skin friction and the local Nusselt number which are defined:

$$C_f = -2\sqrt{\frac{n+1}{2\,\mathrm{Re}_x}}f''(0),\quad \mathrm{Nu} = -\sqrt{\frac{\left(n+1\right)\mathrm{Re}_x}{2}}\theta'(0) \tag{17}$$

where $\mathrm{Re}_x = U_w(x + b)/\nu$ is the local Reynold number [29]. Now, the modified skin-friction is $C_f(\mathrm{Re}_x)^{1/2} = -(2n + 2)^{1/2}f''(0)$ and the modified Nusselt number is $\mathrm{Nu}(\mathrm{Re}_x)^{1/2} = -[(n + 1)/2]^{1/2}\theta'(0)$ [23]. The non-linear differential eqs. (14) and (15) subjected to the boundary conditions (16) are converted into the following simultaneous system of first ODE:

$$y_1' = y_2 \tag{18}$$

$$y_2' = y_3 \tag{19}$$

$$y_3' = \frac{-2(n+1)y_1y_2 + 4ny_2^2 + \beta\left[2(n+1)(1-3n)y_1y_2y_3 + 4n(n-1)y_3^2 - (n^2-1)\eta y_2^2 y_3\right] + 2(n+1)\lambda y_2}{2(n+1) - (n+1)^2\beta y_1^2} \tag{20}$$

$$y_4' = y_5 \tag{21}$$

$$y_5' = -\frac{\left[\dfrac{\Pr}{1+R}\dfrac{y_1y_5 - 2n}{(n+1)y_2y_4}\right] + \varepsilon y_5^2}{1+\varepsilon y_4} \tag{22}$$

where the initial conditions:

$$y_1(0) = \alpha\frac{1-n}{1+n}, \quad y_2(0) = 1, \quad y_3(0) = s_1, \quad y_4(0) = 1 \quad \text{and} \quad y_5(0) = s_2 \tag{23}$$

where s_1 and s_2 are priori unknowns to be determined as a part of the solution. The system of eqs. (18)-(22) subjected to the boundary conditions (23) are solved by fourth/fifth order Runge-Kutta method in combination with shooting method in the symbolic computation software Mathematica as used and explained by Elbashbeshy *et al.* [30].

Results and discussion

To judge the accuracy of our analysis, comparisons are made with variable results corresponding to skin friction coefficient $-f''(0)$ and Nusselt number $-\theta'(0)$ for velocity power index and wall thickness parameter with those of Fang *et al*. [18], Khader and Megahed [19], Salahuddin *et al.* [26], Mabood *et al.* [31], and Wang [32]. The comparisons are presented in tabs. 1 and 2 and it is found that the results are in excellent agreement.

Table 1. A comparison with others for the value of $-f''(0)$ at ($\beta = \lambda = R = 0$), $\varepsilon = 0.1$, Pr = 1, $\eta = 0$ and at different α and n

n	$\alpha = 0.25$			$\alpha = 0.5$		
	[18]	[19]	Present Work	[18]	[19]	Present work
10	1.1433	1.1433	1.14332	1.0603	1.0603	1.06032
9	1.1404	1.1404	1.14039	1.0589	1.0588	1.05891
7	1.1323	1.1322	1.13228	1.0550	1.0551	1.05504
5	1.1186	1.1186	1.11859	1.0486	1.0486	1.04861
3	1.0905	1.0904	1.09049	1.0359	1.0358	1.03586
1	1.0000	1.0000	1.00000	1.0000	1.0000	1.00000
0.5	0.9338	0.9337	0.93382	0.9799	0.9798	0.97994
0	0.78439	0.7843	0.78427	0.9576	0.9577	0.95764
–1/3	0.5000	0.5000	0.50000	1.0000	1.0000	1.00000
–0.5	0.0833	0.0832	0.08333	1.1667	1.1666	1.16666

Table 2. Comparison of $-\theta'(0)$ at different Pr ($\beta = \lambda = R = 0$), $\varepsilon = 0.1$, $n = 1$, $\eta = 0$

Pr	[26]	[31]	[32]	Present work
0.07	0.0654	0.0655	0.0656	0.0656225
0.20	0.1688	0.1691	0.1691	0.1690885
0.7	0.4534	0.4539	0.4539	0.4539165
2.00	0.9108	0.9114	0.9114	0.9113577
7.00	1.8944	1.8954	1.8954	1.8954033
20.00	3.3522	3.3539	3.3539	3.3539043
70.00	6.4619	6.4622	6.4622	6.4621999

The velocity index power n defines the surface shape, the type of motion, and hence the behavior of the boundary-layer. Such as, if $n = 1$, it means that the surface is flat and the boundary-layer is impermeable, if $n < 1$, the thickness decreases with convex outer shape and converted to suction process. For $n > 1$, the surface has increasing thickness with concave outer shape and converted to injection process. On the other hand, for $n = 0$, the motion becomes linear with constant velocity, decelerated for $n < 1$ and accelerated for $n > 1$. Figure 2 shows that the velocity slightly decreases with increasing the velocity power index n and fig. 3 shows that increasing the value of n produces an increase in the temperature profiles. So the larger value of n increases the thermal boundary-layer thickness.

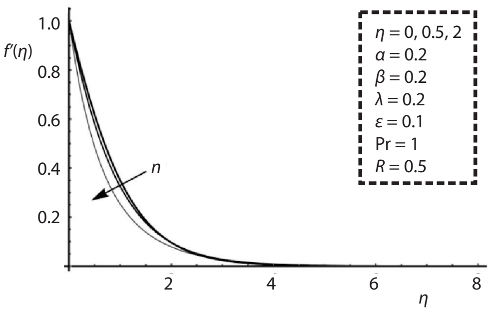

Figure 2. The velocity power index effect on the velocity

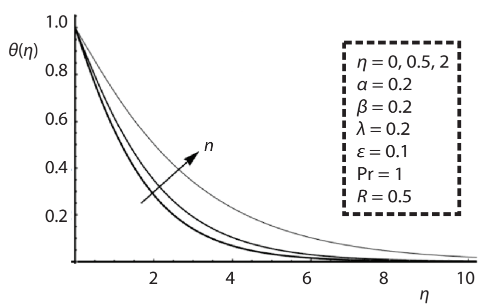

Figure 3. The velocity power index effect on the temperature

From fig. 4, for $n < 1$, as α increases the velocity slightly decreases, consequently, the boundary-layer becomes thinner and thinner, while fig. 5 shows that for $n > 1$ the velocity increases and the boundary-layer becomes thicker.

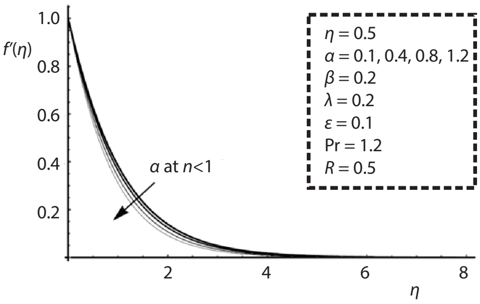

Figure 4. The wall thickness parameter effect on the velocity for $n < 1$

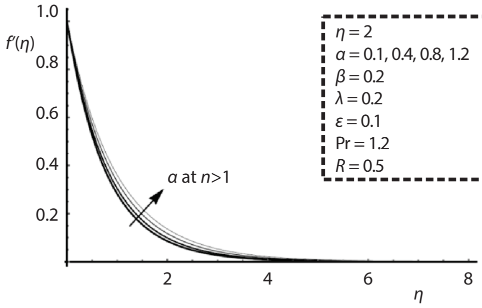

Figure 5. The wall thickness parameter effect on the velocity for $n > 1$

On the other hand, fig. 6 shows that for $n < 1$, as α increases the temperature decreases due to the slowdown in the flow while fig. 7 shows the increase in the temperature with increasing α for $n > 1$. Figure 8 shows that the horizontal velocity decreases with increasing the values of porous parameter λ due to the increase of the pores in the stretched surface. Furthermore, the momentum boundary-layer thickness decreases as porous parameter λ increases while the temperature is enhanced with increasing the porous parameter as shown in fig. 9.

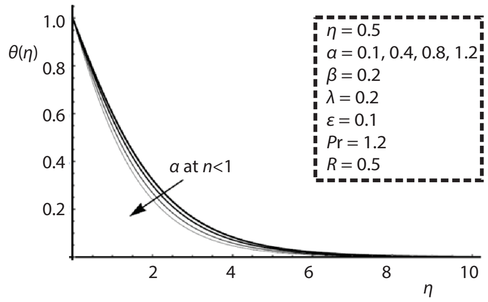

Figure 6. The wall thickness parameter effect on the temperature for n < 1

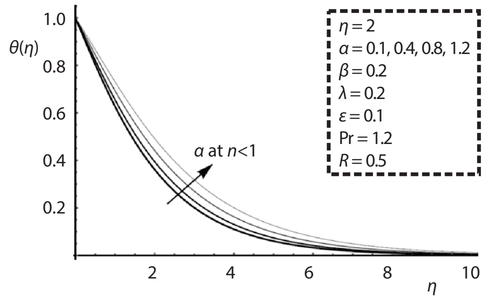

Figure 7. The wall thickness parameter effect on the temperature for n > 1

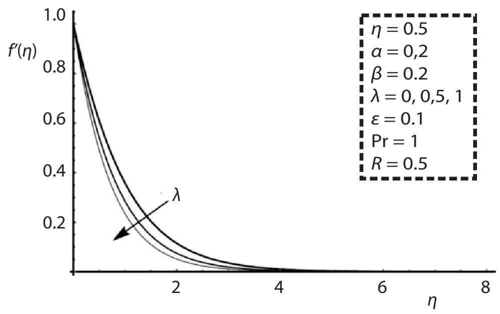

Figure 8. The porous parameter effect on the velocity

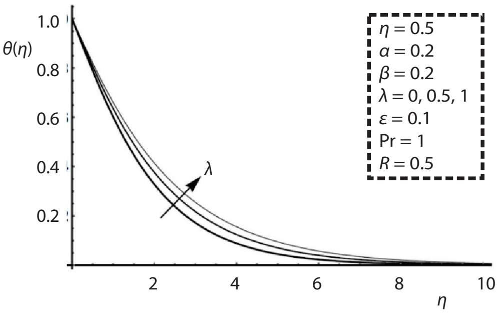

Figure 9. The porous parameter effect on the temperature

Figure 10 shows that increasing the relaxation time, β, reduces the velocity and hence decreases the boundary-layer thickness which in turn increases the temperature as shown in fig. 11. The thermal conductivity is enhanced due to the increase of ε, and then more heat is exchanged between the stretched surface and the adjacent layers of the fluid. This phenomenon in turn explains the increase in the temperature profile as shown in fig. 12.

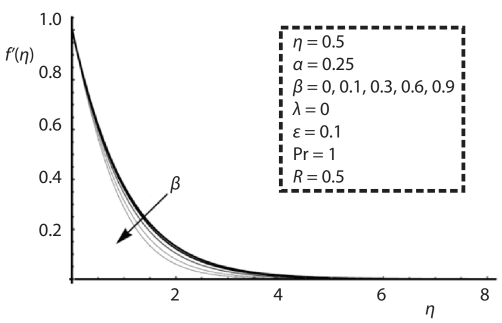

Figure 10. The elasticity number effect on the velocity

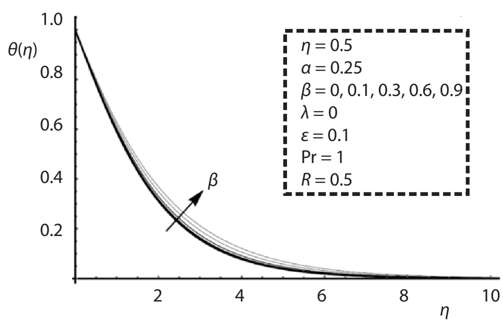

Figure 11. The elasticity number effect on the temperature

From fig. 13, it is observed that increasing Prandtl number decreases the temperature and the thermal boundary thickness. Physically, for higher values of Prandtl number, the thermal diffusivity of the fluid decreases then the fluid has larger heat capacity. The effect of the thermal radiation on the temperature profiles is presented in fig. 14. It is observed that the temperature field and the thermal boundary-layer thickness increase with the increase of the thermal radiation R.

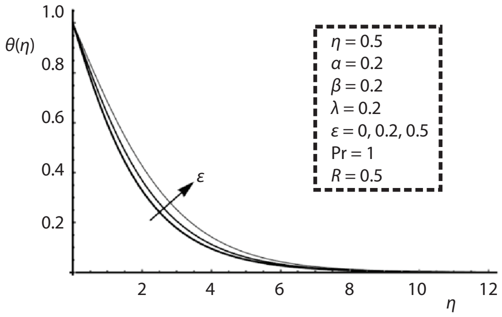

Figure 12. The effect of thermal conductivity parameter ε on the temperature

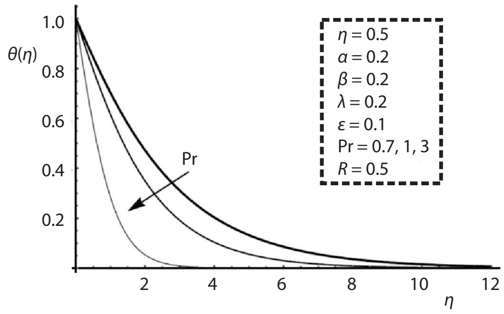

Figure 13. The effect of Prandtl number on the temperature

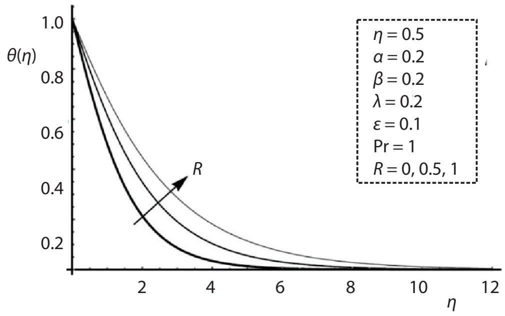

Figure 14. The effect of the radiation parameter on the temperature

Figure 15 shows that the modified skin friction increases with α for the convex surface ($n < 1$) and decreases with α for the concave surface ($n > 1$). Physically, as n increases the flow slow down over the stretching surface causing an increase in the modified skin friction. Finally, the figure shows that for high α the effect of it tends to be one value such as the effect where $n = 1$. Figure 16 shows that the modified Nusselt number increases with $\alpha > 1$ for the convex shape ($n < 1$) and decreases for the concave shape ($n > 1$).

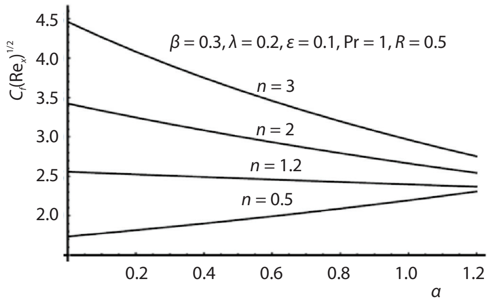

Figure 15. The modified skin-friction *vs.* the wall thickness parameter

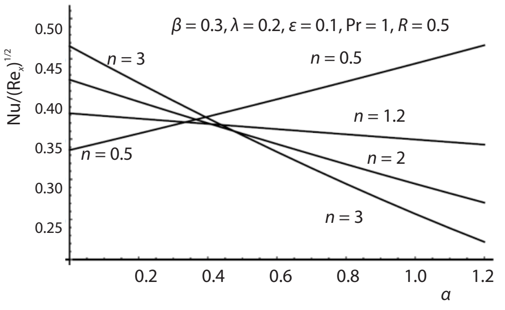

Figure 16. The modified Nusselt number *vs.* the wall thickness parameter

Table 3 presents the values for the modified skin friction coefficient and the modified Nusselt number at different settings. The first part in tab. 3 shows that the modified skin friction increases and the modified Nusselt numbers decreases with increasing the velocity power index. Physically, increasing the power index n increases the effect of the friction between the surface and the adjacent fluid, and increases the heat transfer by conduction. Therefore, the rate of heat transfer from the surface will be decreased, which has a direct negative effect on the mechanical properties of the surface such as hardness, stiffness, strength*, etc.* The second part in tab. 3 shows that increasing the wall thickness parameter α for convex outer shape ($n < 1$) increases the modified skin-friction and Nusselt number while for concave outer surface ($n > 1$) it decreases them, which indicates that the effect of the wall thickness parameter is mainly effected by the surface outer shape.

Table 3. The modified skin-friction and modified Nusselt number at different values of n, α, β, λ, ε, Pr, and R for $\eta = 0$

n	α	β	λ	ε	Pr	R	$C_f(\mathrm{Re}_x)^{1/2}$	$\mathrm{Nu}/(\mathrm{Re}_x)^{1/2}$
–0.5	0.5	0.3	0.2	0.1	1	0.5	1.16246	0.55835
0.5							1.94554	0.38879
1							2.33114	0.37013
0.5	0.2	0.3	0.2	0.1	1	0.5	1.81563	0.35697
0.5	0.5						1.94554	0.38879
5	0.2						5.62450	0.45793
5	0.5						4.63136	0.36017
0.5	0.2	0	0.2	0.1	1	0.5	1.78251	0.36738
		0.9					1.88902	0.33639
		1.4					1.95588	0.32011
0.5	0.2	0.3	0	0.1	1	0.5	1.64029	0.37052
			0.5				2.05252	0.33934
			1				2.39719	0.31549
0.5	0.2	0.3	0.2	0	1	0.5	1.81563	0.38605
				0.2			1.81563	0.33230
				0.5			1.81563	0.27634
0.5	0.2	0.3	0.2	0.1	0.7	0.5	1.81563	0.26848
					3		1.81563	0.78974
					7		1.81563	1.37137
0.5	0.2	0.3	0.2	0.1	1	0	1.81563	0.48515
						1	1.81563	0.28400
						4	1.81563	0.12941

As mentioned before, for high β, the viscosity and resistivity of the fluid are increased inducing more friction within the fluid and reduces the velocity of the flow. These effects appear in increasing the modified skin friction and lowering the modified Nusselt number as tabulated in the third part of tab. 3. The fourth part shows that the modified skin friction increases and the Nusselt number decreases with increasing the porosity parameter λ due to the increase of the pores in the stretched surface as mentioned before. The fifth part shows that the modified Nusselt number decreases with increasing the thermal conductivity parameter ε. Physically, the increase of ε enhances the heat transfer by conduction which reduces the modified Nusselt number. The sixth and seventh parts of tab. 3 show the effect of Prandtl number and the radiation parameter, respectively. For high Prandtl numbers, the modified Nusselt number is high. While, the thermal radiation lowers the modified Nusselt number. The two parameters have no effect on the local skin-friction.

Conclusions

In this study, the flow and heat transfer of the Maxwell fluid over a stretching surface with variable thickness embedded in a porous medium in the presence of thermal radiation is investigated numerically. The key points are summarized below:

- The velocity power index n and the wall thickness parameter α control the mechanical properties of the stretching surface. For $n < 1$, the wall thickness parameter α slightly decreases the velocity and the temperature while, for $n > 1$, it strongly increases them.
- The elasticity parameter β and the porous parameter λ decrease the velocity profile but they increase the temperature profile.
- The temperature distribution increases with increasing the thermal conductivity parameter ε and the thermal radiation parameter, R. But it decreases when Prandtl number increases which in turn reduces the thermal boundary thickness.
- The modified skin-friction $C_f(\mathrm{Re}_x)^{1/2}$ with increasing α (for $n < 1$), β, and λ. While it is decreased with increasing α (for $n > 1$).
- The modified Nusselt number $\mathrm{Nu}/(\mathrm{Re}_x)^{1/2}$ is increased by increasing ε, α (for $n < 1$), and Prandtl number. Whereas increasing n, α (for $n > 1$), β, λ, or R reduces this number.
- The heat transfer is enhanced by increasing the elasticity, the porous, the velocity power index, the thermal conductivity, and the thermal radiation parameters.

Nomenclature

a, b – constants define the wall thickness, [–]
C_p – specific heat at constant pressure, [Jkg^{-1}K^{-1}]
C_f – local skin-friction coefficient, (= $\tau/0.5\rho U_x^2$), [–]
f, F – dimensionless functions, [–]
K – permeability of porous medium, [m^2]
K_{eff} – effective thermal conductivity, [Wm^{-1}K–1]
k – thermal conductivity, [Wm^{-1}K^{-1}]
k^* – mean absorption parameter
Nu – local Nusselt number, [–]
Pr – Prandtl number, (= ν/α), [–]
q_r – radiative heat flux, [Js^{-1}m^{-3}K^{-1}]
R – radiation parameter, [–]
Re_x – local Reynold's number, (= $U_w(x + b)/\nu$), [–]
T – temperature, [K]
U_w – velocity of solid surface, [ms^{-1}]
u, υ – velocity components along x and y, [ms^{-1}]
x, y – axes of the surface, [m]

Greek symbols

α – wall thickness parameter, [–]
β – elasticity parameter, [–]
ε – thermal conductivity parameter, [–]
η, ξ – dimensionless co-ordinates, [–]
θ – dimensionless temperature, [–]
λ – porosity parameter, [–]
λ_1 – relaxation time of the fluid, [–]
ν – kinematical viscosity, (= μ/ρ), [m^{2}s^{-1}]
ρ – fluid density, [Kgm^{-3}]
μ – dynamical viscosity, [Kgm^{-1}s^{-1}]
σ^* – Stefan-Boltzmann constant, [Wm^{-2}K^{-4}]
ψ – physical stream function, [m^{2}s^{-1}]

Subscripts and superscript

w – condition on the wall
∞ – free stream condition
n – velocity power index, [–]

References

[1] Sakiadis, B. C., Boundary-Layer Behavior on Continuous Solid Surfaces: II Boundary-Layer on a Continuous Flat Surface, *American Institute of Chemical Engineers Journal*, *7* (1961), 2, pp. 221-225
[2] Crane, L. J., Flow Past a Stretching Plate, *Z. Angew. Math. Phys*., *21* (1970), 4, pp. 645-647
[3] Elbashbeshy, E. M. A., Bazid, M. A. A., Heat Transfer over a Continuously Moving Plate Embedded in Non-Darcian Porous Medium, *International Journal of Heat and Mass Transfer*, *43* (2000), 17, pp. 3087-3092
[4] Hossain, M. A., *et al.*, The Effect of Radiation on Free Convection Flow of Fluid with Variable Viscosity from a Porous Vertical Plate, *Int. J. Therm. Sci*., *40* (2001), 2, pp. 115-124
[5] Cortell, R., Flow and Heat Transfer of a Fluid through a Porous Medium over a Stretching Surface with Internal Heat Generation/Absorption and Suction/Blowing, *Fluid Dynamics Research*, *37* (2005), 4, pp. 231-245

[6] Yusof, Z. M., *et al.*, Radiation Effect on Unsteady MHD Flow over a Stretching Surface, *International Journal of Computer, Electrical, Automation, Control and Information Engineering*, *6* (2012), 12, pp. 1772-1775
[7] Elbashbeshy, E. M .A., *et al.*, Effects of Thermal Radiation and Magnetic Field on Unsteady Mixed Convection Flow and Heat Transfer over an Exponentially Stretching Surface with Suction in the Presence of Internal Heat Generation/Absorption, *Journal of the Egyptian Mathematical Society*, *20* (2012), 3, pp. 215-222
[8] Mandal, C., Swati M., Heat Transfer Analysis for Fluid-Flow over an Exponentially Stretching Porous Sheet with Surface Heat Flux in Porous Medium, *Ain Shams Engineering Journal*, *4* (2013), 1, pp. 103-110
[9] Elbashbeshy, E. M. A., *et al.*, Unsteady Flow of Micropolar Maxwell Fluid over Stretching Surface in The Presence of Magnetic Field, *International Journal of Electronic Engineering and Computer Science*, *2* (2017), 4, pp. 28-34
[10] Hsiao, K. L., Combined Electrical MHD Heat Transfer Thermal Extrusion System Using Maxwell Fluid with Radiative and Viscous Dissipation Effects, *Applied Thermal Engineering*, *112* (2017), Feb., pp. 103-110
[11] Hsiao, K. L., To Promote Radiation Electrical MHD Activation Energy Thermal Extrusion Manufacturing System Efficiency by Using Carreau-Nanofluid with Parameters Control Method, *Energy*, *130* (2017), July, pp. 486-499
[12] Shehzad, S. A., *et al.*, Radiative Maxwell Fluid-flow with Variable Thermal Conductivity due to a Stretching Surface in a Porous Medium, *Journal Aerosp. Eng*., *27* (2014), 5
[13] Waheed, S. E., Flow and Heat Transfer in a Maxwell Liquid Film over an Unsteady Stretching Sheet in a Porous Medium with Radiation, *Waheed Springer Plus*, *5* (2016), 1, pp. 2-14
[14] Noor, N. F. M., *et al.*, Heat Flux Performance in a Porous Medium Embedded Maxwell Fluid-Flow over a Vertically Stretched Plate Due to Heat Absorption, *Journal Non-linear Sci. Appl.*, *9* (2016), 5, pp. 2986-3001
[15] Hsiao, K. L., Micropolar Nanofluid-Flow with MHD and Viscous Dissipation Effects Towards a Stretching Sheet with Multimedia Feature, *International Journal of Heat and Mass Transfer*, *112* (2017), Sept., pp. 983-990
[16] Hsiao, K. L., Stagnation Electrical MHD Nanofluid Mixed Convection with Slip Boundary on a Stretching Sheet, *Applied Thermal Engineering*, *98* (2016), Apr., pp. 850-861
[17] Hsiao, K. L., Corrigendum to ‘Stagnation Electrical MHD Nanofluid Mixed Convection with Slip Boundary on a Stretching Sheet, *Applied Thermal Engineering*, *125* (2017), Oct., p. 1577
[18] Fang, T., *et al.*, Boundary-Layer Flow over a Stretching Sheet with Variable Thickness, *Applied Mathematics and Computation*, *218* (2012), 13, pp. 7241-7252
[19] Khader, M. M., Megahed, A. M., Numerical Solution for Boundary-Layer Flow Due to a Non-Linearly Stretching Sheet with Variable Thickness and Slip Velocity, *Eur. Phys. J. Plus*, *128* (2013), 9, pp. 1-7
[20] Khader, M. M., *et al.*, Numerical Study for Simulation the MHD Flow and Heat transfer Due to a Stretching Sheet on Variable Thickness and Thermal Conductivity with Thermal Radiation, *Applied Mathematics*, *6* (2015), 12, pp. 2045-2056
[21] Eid, A., Khader, M. M., Numerical Studies Using Finite different Method for Viscous Dissipation and Thermal Radiation Effects on the Slip Flow and Heat Transfer Due to a Stretching Sheet Embedded in a Porous Medium with Variable Thickness and Variable Thermal Conductivity, *NTMSCI*, *4* (2016), 1, pp. 38-50
[22] Elbashbeshy, E. M. A., *et al.*, Flow and Heat Transfer over a Moving Surface with Non-Linear Velocity and Variable Thickness in a Nanofluid in the Presence of Thermal Radiation, *Can. J. Phys*., *92* (2014), 2, pp. 124-130
[23] Abdel-Wahed, M. S., *et al.*, Flow and Heat Transfer over a Moving Surface with Non-Linear Velocity and Variable Thickness in a Nanofluids in the Presence of Brownian Motion, *Applied Mathematics and Computation*, *254* (2015), Mar., pp. 49-62
[24] Sulochana, C., Sandeep, N., Dual Solutions for Radiation MHD Forced Convective Flow of A Nanofluid over A Slandering Stretching Sheet in Porous Medium, Journal of Naval Architecture and Marine Engineering, *Journal of Naval Architecture and Marine Engineering*, *12* (2015), 2, pp. 115-124
[25] Hayat, T., *et al.*, Impact of Cattaneo-Christov Heat Flux in the Flow over a Stretching Sheet with Variable Thickness, *AIP ADVANCES*, *5* (2015), 8, pp. 1-12
[26] Salahuddin, T., *et al.*, MHD flow of Cattanneo-Christov Heat Flux Model for Williamson Fluid over a Stretching Sheet with Variable Thickness: Using Numerical Approach, *Journal of Magnetism and Magnetic Materials*, *401* (2016), Mar., pp. 991-997

[27] Raptis, A., Flow of a Micropolar Fluid Past a Continuously Moving Plate by the Presence of Radiation, *Int. J. of Heat Mass Transfer*, *41* (1998), 18, pp. 2865-2866
[28] Raptis, A., Radiation and Viscoelastic Flow, *Int. Com. Heat Mass Transfer*, *26* (1999), 6, pp. 889-895
[29] Khader, M. M., Megahed, A. M., Approximate Solutions for the Flow and Heat Transfer due to a Stretching Sheet Embedded in a Porous Medium with Variable Thickness, Variable Thermal Conductivity and Thermal Radiation Using Laguerre Collocation Method, *Applications and Applied Mathematics: An International Journal*, *10* (2016), 2, pp. 817-834
[30] Elbashbeshy, E. M. A., *et al.*, Effect of Thermal Radiation on Flow, Heat, and Mass Transfer of a Nanofluid over a Stretching Horizontal Cylinder Embedded in a Porous Medium with Suction/Injection, *Journal of Porous Media*, *18* (2015), 3, pp. 215-229
[31] Mabood, F., *et al.*, MHD Boundary-Layer Flow and Heat Transfer of Nanofluids over a Non-Linear Stretching Sheet: A Numerical Study, *Journal of Magnetism and Magnetic Materials*, *374* (2015), Jan., pp. 569-576
[32] Gorla, R. S. R., Sidawi, I., Free Convection on a Vertical Stretching Surface with Suction and Blowing, *Appl. Scientific Research*, *52* (1994), 3, pp. 247-257

Paper submitted: February 28, 2017
Paper revised: February 4, 2018
Paper accepted: May 2, 2018